PHASE I CLINICAL TESTING AND IMMUNE CHARACTERIZATION OF AN ADIPOSE EXTRACELLULAR MATRIX DERIVED BIOMATERIAL FOR SOFT TISSUE RECONSTRUCTION

by
Alexis Parrillo

A thesis submitted to Johns Hopkins University in conformity with the requirements for the degree of Master of Science in Engineering.

Baltimore, Maryland
May 2017

ABSTRACT

An adipose extracellular matrix derived biomaterial, Acellular Adipose Tissue, can be used as an off-the-shelf alternative to autologous fat transfer for the treatment of soft tissue deformities and defects. This tissue engineering solution overcomes many challenges associated with autologous fat transfer and other common methods of soft tissue reconstruction. Subcutaneous Acellular Adipose Tissue implants display significant volume retention with minimal inflammatory response in both pre-clinical and clinical studies. The material triggers cell migration which supports development of new adipose and has also demonstrated the potential to modulate the immune response to create a more pro-regenerative microenvironment in the presence of trauma. These results indicate that Acellular Adipose Tissue could be a promising new therapeutic tool to treat soft tissue defects and promote wound healing.

Advisor: Jennifer Elisseeff, Ph.D.

Readers: Warren Grayson, Ph.D.
Alexander Hillel, M.D.

ACKNOWLEDGEMENTS

I would like to acknowledge all of the many individuals who helped make this work possible. I am extremely thankful for every member of the Elisseeff lab who trained and guided me throughout my Master's degree, especially Amy Anderson and Matt Wolf for answering my never-ending questions and always making me feel comfortable going to them for support. Thank you to Bahar Zarrabi for always having her door open, both when I needed an administrator and when I needed a friend. I don't know where I would be without her endless support! I also would like to acknowledge the people who helped make the clinical trial possible, including our team of physicians and trial managers. And of course, thank you to my friends and family for their endless love and support.

My advisor, Dr. Jennifer Elisseeff, has provided so much guidance and helpful input throughout my Master's program. Her direction of this project and help thinking through the tough questions has been invaluable. I have also appreciated her willingness to allow me to work on projects, sit in on phone calls, and pursue topics that aligned with my interests. Her guidance throughout my Master's has helped me to develop into the scientist, engineer, and person that I am. I have enjoyed working with her tremendously, and I appreciate all of the opportunities that she has given me.

Amy Anderson has been my partner and friend throughout my entire program, and I would not have made it through without her. All of the work in this thesis belongs to her as much as it does to me. Being able to work with her made me enjoy coming to the lab every single day (even the early ones). Somehow, we were still laughing together even at the end of a fifteen-hour day. I have learned so much about being a scientist from her, and I cannot thank her enough for everything that she has taught me.

TABLE OF CONTENTS

LIST OF FIGURES

LIST OF TABLES

TABLE OF ABBREVIATIONS

AAT	Acellular Adipose Tissue
ANOVA	Analysis of Variance
ASC	Adipose-derived stem cell
bFGF	Basic fibroblast growth factor
cDNA	Complementary deoxyribonucleic acid
DAMP	Damage associated molecular patterns
DMAB	4-(Dimethylamino)benzaldehyde
DPBS	Dulbeccos' phosphate buffered saline
ECM	Extracellular Matrix
EDTA	Ethylenediaminetetraacetic acid
FBS	Fetal bovine serum
GMP	Good manufacturing practices
H&E	Hematoxylin and Eosin
hAAT	Human acellular adipose tissue
HLA	Human leukocyte antigen
HPLC	High-performance liquid chromatography
IACUC	Institutional Care and Use Committee
IgG	Immunoglobulin G
mAAT	Mouse acellular adipose tissue
pAAT	Porcine acellular adipose tissue
PRA	Panel-reactive antibody
PCR	Polymerase chain reaction
qPCR	Quantitative PCR
RNA	Ribonucleic acid
RT	Reverse transcriptase
SAE	Serious adverse event
SQ	Subcutaneous
VML	Volumetric muscle loss

INTRODUCTION

Soft tissue defects are relatively common and can occur due to trauma, congenital disease, or surgical inventions. As tissue loss is often permanent, these defects can impact not only cosmesis but also normal physiological function, including lack of support for distal extremities and contracture leading to restricted range of motion [1]. The gold standard for soft tissue reconstruction is autologous adipose transfer (otherwise known as fat grafting), a procedure first developed by Gustav Neuber over a century ago [2, 3]. However, although these procedures are still commonly used today and many advancements have been introduced, autologous fat transfer techniques have many limitations. Adipose grafts behave unpredictably and outcomes can often vary significantly from patient to patient. The grafted tissue can be resorbed anywhere from 20%-90%, decreasing the total volume of the graft and often requiring multiple surgical procedures to achieve the desired correction. Like any surgical procedure, autologous fat grafting carries inherent safety risks. The unpredictability of these procedures can result in costly surgeries and co-morbidities related to tissue harvest. Harvest procedures often lead to scarring at the donor site and are limited by the volume of autologous tissue available in each patient [4]. Transplanted adipocytes are often damaged or subjected to hypoxic conditions that result in the release of intracellular lipids, a potent pro-inflammatory signal. These signals combined with a lack of vascularization within the graft can lead to tissue necrosis and calcifications which impact the quality and durability of the reconstructed tissue [5].

Decellularized extracellular matrix (ECM) products are a type of biomaterial that have recently gained popularity in the field of regenerative medicine, although they have

been studied and used in various clinical applications since as early as 1995 [6]. Unlike synthetic biomaterials such as polymers, ECM materials are tissue-derived and are created using physical, enzymatic, and chemical approaches that remove the living cells from almost any type of animal or human tissue [7]. These decellularization processes disrupt cellular membranes and denature key intracellular components such as DNA, but leave behind the non-cellular component which is present in all tissues and organs. This non-cellular component is mainly structural in nature and is known as the extracellular matrix (ECM). Although all ECMs are composed of water, proteins, and polysaccharides, the physical characteristics and exact composition of any specific ECM depends on its tissue of origin. ECMs have many physiological roles, including providing a physical scaffold and initiating cues required for tissue homeostasis and differentiation. ECM also directs function by binding to growth factors and interacting with receptors on the cell surface [8].

ECM scaffolds are commonly used in tissue engineering to promote the healing or regrowth of damaged tissue. Initially, they provide a physical substrate upon which the cells can be seeded and localized to a specific area. They also provide key biochemical and physical cues for adhesion, migration, proliferation, and differentiation which help cells to form fully functional tissues or organs. Implanted ECM scaffolds will eventually be remodeled and be replaced with the seeded cells' own secreted matrices.

ECM has many beneficial uses and new applications that are currently being explored in regenerative medicine. In the past 15 years, many ECM materials have been brought to market and been successfully used clinically. Alloderm®, an ECM product, has been used for dentistry, burn therapy, plastic surgery, and hernia repair for over 13

years. Many decellularized bone allografts have also been successfully marketed and used clinically for bone reconstruction. In one case, a complicated scaffold made of porcine small intestinal sub-mucosa ECM was used to treat a quadriceps defect in a 19-year-old marine three years post-injury, resulting in remarkable improvement after only 4 months [9]. The complex protein and polysaccharide composition and unique physical structures of an ECM cannot be mimicked using any synthetic biomaterial currently available, and thus these biomimetic scaffolds effectively modulate signal transduction and both directly and indirectly regulate cellular function similar to natural ECM [10]. The remarkable successes of ECM products already on the market and the potential benefits of ECM materials due to their biomimetic properties indicate that the possible clinical applications of these materials are vast.

Adipose tissue is where the body stores excess energy and regulates metabolic homeostasis by synthesizing and secreting various compounds. It is made up mostly of adipocytes, but also consists of blood cells, endothelial cells, adipose precursor cells, pericytes, and other cells in the stromal vascular fraction. Adipocytes can increase primarily in size but also in number in order to store excess energy produced from food [11]. Adipose is also a robust source of mesenchymal stem cells, called adipose-derived stem cells (ASCs), which have the potential to differentiate into multiple lineages [12].

As per their role as energy suppliers for the body, adipose cell signaling can have a significant impact on overall health. It has been noted clinically that transplanting autologous fat can have a positive impact on surrounding tissues. This includes improvements in both scarring and aging skin. Perhaps more strikingly, autologous fat transfers have also improved radiation damage, damaged vocal cords, and chronic

ulceration. These improvements may be related to undifferentiated cells, such as ASCs, in the adipose tissue [13]. These clinical observations indicate an important connection between adipose tissue and wound healing.

Adipose tissue is a practical raw material source for producing ECM biomaterials for several reasons. To start, adipose is relatively abundant and easy to harvest, whether from a deceased tissue donor or in a minimally invasive procedure for autologous use. An adult human can have a body fat composition of anywhere from less than 10% (a lean individual) to more than 50% (an obese individual) [14]. Additionally, adipose contains secreted factors that are beneficial for angiogenesis, anti-inflammation, and anti-apoptosis [15, 16]. Importantly, adipose tissue can also play a role in immune modulation. The metabolic processes carried out by adipose tissue, including adipocyte expansion and thermogenesis, can activate both the adaptive and innate immune system [17]. All of these qualities of adipose tissue make it an ideal candidate for a decellularized ECM biomaterial for use in wound healing and reconstruction applications.

When addressing the challenges of wound healing and reconstruction, it is important to understand the role of the immune system. Immune cells are important in every step of the wound healing process, from debridement to new tissue and scar formation. Neutrophils arrive at the wound site about 24 hours after injury. Their main role is to debride the wound and decrease the likelihood of infection. Approximately 48-96 hours after injury, macrophages migrate in and promptly become the predominant cell population. They contribute to and conclude wound debridement and secrete cytokines and growth factors that play a key role in cell recruitment and regulation during tissue

repair, including both angiogenesis and new matrix deposition. On approximately the fifth day following injury, T lymphocytes migrate into the wound and regulate the proliferation phase of tissue repair [18].

As the immune system's contribution to and regulation of tissue development and regeneration is becoming better understood [19], tissue engineers are beginning to realize that it is important to approach regeneration with the immune system in mind. Recent studies have identified the role of T helper 2 cells in the biomaterial scaffold directed tissue repair [20] and examined the role of macrophages in the remodeling process after implantation of a surgical mesh [21]. It is also important to note that macrophage phenotype plays a key role in wound healing. Macrophages exist on a spectrum ranging from "M1 macrophages" which are typically described as pro-inflammatory to "M2 macrophages" which are considered regulatory or homeostatic [21]. Macrophage heterogeneity [22] and its implications for wound healing [23] can have a huge impact on the design of biomaterials to elicit pro-regenerative responses.

The work in this thesis describes the immunological characterization and Phase I clinical testing of an adipose extracellular matrix product, called Acellular Adipose Tissue (AAT). This product was developed at Johns Hopkins University in the laboratory of Dr. Jennifer Elisseeff and is intended to fill the clinical need for an "off-the-shelf" soft tissue repair technology for volume augmentation and soft tissue reconstruction. AAT provides a structure that mimics normal soft tissue and a matrix to promote cell migration and new fat tissue growth. Extensive preclinical studies have characterized the physical properties and evaluated compatibility and efficacy in vivo [24, 25], including an evaluation of new adipose tissue development in athymic mice and biocompatibility in

immune competent rodents. The *in vivo* behavior of the AAT was evaluated in multiple animal models including mouse, rat, and swine in comparison to the current clinical gold standard of autologous fat grafting. Overall, these results highlight the biocompatibility of the AAT implants and their ability to provide soft tissue volume replacement. They also show an advantage autologous fat grafting which may cause calcification due to an inflammatory response to released intracellular lipids [3, 26].

Studies done by Dr. Elisseeff and the Biomaterials and Tissue Engineering Lab at Johns Hopkins investigating the immunological profile of various ECM-derived scaffolds [20] suggest that the constituents of an ECM scaffold can alter the immune microenvironment of the tissue. These studies establish a critical role for the local immunological microenvironment in wound healing and suggest that the immune-modulating properties of ECM-based biomaterials such as AAT may be used in a targeted manner to facilitate wound healing. Human clinical studies and animal research aimed to investigate the immunocomposition of AAT and determine the resulting impact on wound healing and tissue regeneration.

METHODS

ECM production

Human cadaveric adipose tissue was obtained from Donor Network West and shipped to Johns Hopkins at -20˚C. Porcine adipose tissue was obtained from Wagner Meats and delivered to Johns Hopkins at 4˚C and stored at -20°C. Tissue was thawed at room temperature immediately prior to use (porcine tissue was warmed to 37˚C in a water bath prior to processing). The tissue was dissected into 1 cm^3 pieces and mechanically pressed until all lipids were removed. The tissue was then incubated in 3% peracetic acid for 3 hours at room temperature stirred at 300 RPM. The tissue was rinsed with Dulbecco's phosphate buffered saline (DPBS) + HEPES buffer six times and then pH tested. Once the pH became neutral (7 or greater), tissue was incubated in Triton X-100/ethylenediaminetetraacetic acid (EDTA) overnight at room temperature with continuous stirring at 300 RPM. The following day, the treated tissue was rinsed in DPBS until no bubbles appeared upon agitation. Water was then pressed out of the tissue and the moisture content was analyzed. The tissue was then knife milled and DPBS was added until the moisture content was 91% (± 1%). The final ECM product is stored in capped 5 mL syringes at 4˚C for up to 1 year. All processing is done in a biosafety cabinet to ensure sterility. The clinical lot was manufactured at the Johns Hopkins Cell Therapy Laboratory's GMP manufacturing facility in accordance with good manufacturing practices (GMP).

In preclinical studies, several lots of human adipose-derived AAT (hAAT) and one lot of porcine adipose-derived AAT (pAAT) were assessed. A single lot of GMP-manufactured

hAAT was used in Phase I clinical testing (TS-0680). Biochemical characterization studies were performed on the GMP-manufactured hAAT clinical lot (TS-0268) and a second non-GMP hAAT batch that was manufactured sterilely in a biosafety cabinet according to Good Laboratory Practices (TS-0267). A pAAT batch was also manufactured sterilely in the lab according to the same protocol (PA1). All *in vivo* animal studies were performed using the hAAT lab batch (TS-0267) and the pAAT lab batch (PA1). Unlike the clinical lot, the two non-GMP batches used in animal testing were not terminally sterilized by gamma irradiation, though sterility was carefully maintained.

VML Surgeries

Animals were anesthetized using 4% isoflurane and maintained during the surgery using 2.5% isoflurane. Hair was removed at the surgical site, and the area was sterilized with 70% ethanol. An incision was created from just above the knee to the hip. A 3 mm x 3 mm defect was created in the quadricep muscle using surgical scissors. The defect was filled with 0.05 cc of either ECM material or sterile DPBS (Gibco) as a control. The incision was closed using 3-5 sterilized wound clips (Roboz Surgical). Immediately following surgery, animals received carprofen (Rimadyl, Zoetis) subcutaneously at 5 mg/kg for pain. Animals were then monitored until waking. At the desired study end points (1, 3, or 6 weeks), animals were sacrificed and both quadriceps and all inguinal (local) lymph nodes, and axillary / brachial (distal) lymph nodes were removed. All samples designated for gene expression analysis were immediately transferred into RNAlater (ThermoFisher), stored at 4˚C for 24 hours, and then moved to -80˚C if ribonucleic acid (RNA) isolations were not to be performed immediately. Quadriceps for

flow cytometry analysis were processed immediately after removal. All animal procedures were performed in accordance with protocols approved by Johns Hopkins Institutional Care and Use Committee (IACUC).

Subcutaneous Injections

Animals were anesthetized using 4% isoflurane and maintained during the surgery using 2.5% isoflurane. The area was sterilized using 70% ethanol. Animals received two 0.20 cc injections of ECM into the subcutaneous space at superior and inferior positions on the dorsal side of the animal. Animals were then monitored until waking. At desired study end points (1 or 3 weeks), animals were sacrificed and samples were collected (implants and inguinal, axillary, and brachial lymph nodes). For flow cytometry and gene expression analysis, any skin was cut away from the implant. For histology, skin and implant were harvested together.

Flow cytometry

Harvested animal or human tissue was finely diced in 1X DPBS on ice. Diced tissue was then digested in an enzyme solution consisting of 1.67 Wunsch U/ml Liberase TL (Sigma-Aldrich) and 0.2 mg/ml DNAse I (Roche) in serum-free RPMI 1640. Digested tissue was then filtered sequentially through 100 μm and 70 μm filters. Cells were then pelleted at 4°C at 300xg for 10 minutes. In some cases, the cell pellets were enriched for hematopoietic cells using Lympholyte (Cedarlane) reagent. Remaining cells were then washed in DPBS (300xg for 5 minutes), then resuspended in a viability dye and stained for 30 minutes on ice, then washed, then stained 45 minutes on ice with the flow

cytometry antibody mixtures (see panel summary in Tables 1 and 2 below). Stained cells were then washed and fixed using Cytofix (BD Biosciences), then washed and stored in DPBS for up to 24 hours prior to data acquisition. Data was obtained using an LSR II flow cytometer (BD Biosciences) and analysis was conducted with FlowJo software.

Table 1. Mouse flow cytometry panel for subcutaneous injection studies

Conjugate	Antigen	Phenotype	Staining Dilution
AF488	CD3	T cells	1:250
BV421	CD19	B cells	1:400
PE-Cy7	F4/80	Macrophages	1:250
APC-Cy7	CD11c	Dendritic cells	1:200
AF700	CD86	M1 macrophages	1:200
APC	CD206	M2 macrophages	1:400

Table 2. Mouse flow cytometry panel for volumetric muscle loss studies

Conjugate	Antigen	Phenotype	Staining Dilution
PerCP/Cy5.5	CD11c	Dendritic cells	1:100
PE-Cy5	CD3	T cells	1:200
PE-594 (CF)	Siglec-F*	Eosinophils	1:200
PE	CD206	M2 macrophages	1:250
Pacific Blue	Ly6g	Neutrophils	1:400
PE-Cy7	F4/80	Macrophage	1:250
APC	CD86	M1 macrophages	1:400
BV605	CD45	Hematopoetic cells	1:150
AF488	MHCII I-A/I-E	Antigen presentation	1:200
AF700	CD11b	Myeloid cell	1:400
BV510	Ly-6C	Monocytes	1:300

Unless otherwise noted, all antibodies were obtained from Biolegend. Antibodies marked with (*) were obtained from BD Biosciences.

RT-qPCR

Tissue was thawed and removed from RNAlater, rinsed in PBS and then homogenized in TRIzol (Life Technologies) using fine scissors and RNase-free pestles. RNA was isolated by chloroform extraction, then the aqueous layer containing RNA was transferred to a

fresh tube containing an equal volume of 70% ethanol. The mixture was then applied to RNeasy Mini columns (Qiagen) and purified according to the manufacturer's instructions. RNA was eluted in RNase-free water and quantified using a Qubit 2.0 fluorometer (Invitrogen). RNA was treated to remove residual DNA using a cocktail containing DNase I, 10x DNase buffer and RNaseOUT inhibitor according to reagent protocols (Life Technologies). Complementary deoxyribonucleic acid (cDNA) synthesis was conducted using Superscript Reverse Transcriptase (RT) III enzyme as per manufacturer's instructions (Life Technologies). Real time quantitative polymerase chain reaction (qPCR) was conducted on Applied Biosystems Real Time PCR machines using SYBR Green as a reporter. Primer sequences are included in Table 3.

Table 3. Real time quantitative PCR Primer Sequences

Gene	Forward Primer (5' → 3')	Reverse Primer (5' → 3')
Arg1	ACAAGACAGGGCTCCTTTCAG	TAAAGCCACTGCCGTGTTCA
Retnlα	CAGCTGATGGTCCCAGTGAAT	AGTGGAGGGATAGTTAGCTGG
Tnfα	ATGGCCTCCCTCTCATCAGT	TGGTTTGCTACGACGTGGG
Il-4	GGTCACAGGAGAAGGGACGC	AGCACCTTGGAAGCCCTACA
Il-10	CAGGACTTTAAGGGTTACTTGGGT	GCCTGGGGCATCACTTCTAC
Il-1β	TGCCACCTTTTGACAGTGATG	AAGCTGGATGCTCTCATCAGG
iNos	CTTGGTGAAGGGACTGAGCTG	GTTCTCCGTTCTCTTGCAGTTG
Ifnγ	CGGCACAGTCATTGAAAGCC	TGTCACCATCCTTTTGCCAGT
Gata3	CTCCTTGCTACTCAGGTGATCG	AGGGAGAGAGGAATCCGAGT
B2m	CACTGAATTCACCCCCACTGA	TCTCGATCCCAGTAGACGGT

Histology

Samples were fixed in 10% formalin, serially dehydrated in graded ethanol solutions, and embedded in paraffin. Microtome sectioning was performed to obtain sections of 5 μm thickness. Slides were stained using a standard Hematoxylin and Eosin (H&E) staining protocol or a Modified Masson's Trichrome protocol.

Functional Testing

Animals were trained on the treadmill apparatus 48 hours prior to testing. During the training, the treadmill was set to 5 m/min and increased by 1 m/min every minute for 5 minutes. During testing, mice were run to exhaustion starting at a speed of 5 m/min and increased by 1 m/min every minute. The mice were considered exhausted when they remained on the pulsed shock grid for 30 continuous seconds. All treadmill testing was done at least 48 hours prior to the study end points where tissue samples were collected.

Clinical Trial

Eight healthy volunteers were injected with AAT in redundant tissue previously scheduled for surgical removal in an elective surgical procedure (i.e. panniculectomy, abdominoplasty). Each patient received a total of 2 mL of AAT in one (2 mL injection) or two injection sites (1 mL injection). Participants had follow-up visits at 1, 2, and 4 weeks post-injection (if implant has not yet been excised) and 2 and 6 weeks post-excision. Pain and itching were assessed at all follow-up visits. Implants were excised during an elective surgical procedure after 1, 2, 4, 6 or 18 weeks *in situ* and delivered to the lab (tissue was transported on 4°C gel packs if travel time exceeded 20 minutes). Tissue samples were photographed, dissected, weighed, and transferred to the appropriate storage or processing reagent for downstream analysis. Panel-reactive antibody testing at 4 and 12 weeks post injection (independent of the excision time-point) indicated if the patient had experienced a systemic human leukocyte antigen (HLA) antibody reaction to the material.

Cell Migration Assay

AAT-triggered cell migration was measured using a transwell assay relative to several control solutions: 10% fetal bovine serum (FBS) in serum free media for a positive control, 1% PBS in serum free media for a buffer control, and serum free media alone for a negative control. Human adipose-derived stem cells (ASCs) were thawed and grown in basic growth media supplemented with 1 ng/mL basic fibroblastic growth factor (bFGF) and passaged and split once at approximately 80% confluency, with media changes every 2-3 days. Upon reaching 80% confluency a second time, cells were serum starved for 24 hours prior to performing assay. After starvation, cells were trypsinized and a single cell suspension was created at 300,000 cells/mL in serum free media. Sample was prepared by adding AAT to serum free media at a 1% (v/v) concentration and vortexing. In some assays, samples incubated at room temperature for 15 minutes and centrifuged to remove large chunks of AAT that might stick to the transwell membrane. Sample, 10% FBS, 1% buffer and serum free media (600 µl) were added in triplicate wells of a 24 well plate, a transwell insert was placed on top, and the plate was allowed to acclimate in an incubator. After acclimation, 100 µL of the cell suspension was added into the upper chamber of each transwell (300,000 cells per well) and incubated at 37˚C for 6 hours. All cells remaining on the upper side of the membrane were removed using a cotton swab and any excess AAT was removed from the lower membrane by rinsing in DPBS. Transwells were fixed in methanol for 15 minutes at room temperature, stained with DAPI, and then imaged within 72 hours. Cell nuclei were counted in a 50x field of view. Cell migration was calculated relative to positive and negative control groups.

Lipid Content

The total lipid content of biomaterials was quantified using a triglyceride colorimetric assay. Adipose samples and AAT were minced into 1 mm or smaller pieces to disrupt physical barriers and release lipids. Organic extraction was conducted by the Schwartz method and enzymatic reactions were carried out using Infinity TG Reagent according to the manufacturer's protocol. Absorbance was measured at 540 nm and concentration of the samples was determined using a glycerol standard curve (samples prepared in water).

Collagen Content

Since hydroxyproline is largely restricted to collagen, the measurement of hydroxyproline levels can be used as an indicator of collagen content. In this assay, hydroxyproline concentration is determined by a reaction of oxidized hydroxyproline with 4-(Dimethylamino)benzaldehyde (DMAB), which results in a colorimetric (560 nm) product, proportional to the hydroxyproline present. Sample preparation consisted of lyophilization and hydrochloric acid hydrolysis of 10 mg of sample (dry weight) at 120˚C for 3 hours. The hydrolyzed samples were diluted 100x and added in triplicate to a 96 well plate in multiple dilutions, along with samples for a hydroxyproline standard curve. A spiked control was also used to detect any interfering endogenous compounds. All wells in the plate were evaporated to dryness. The colorimetric reaction was carried out using reagents provided in the Hydroxyproline Assay Kit (Sigma) according to the manufacturer's instructions. Absorbance was measured at 560 nm and the standard curve was used calculate hydroxyproline content of unknown samples.

Residuals Testing

A batch of AAT was manufactured without EDTA or Triton-X100 to serve as a negative control in the development of these assays. To determine the amount of residual EDTA in the clinical AAT lot, a semi-quantitative method was developed using Quantofix EDTA test strips. The test method was validated using standard solutions of known EDTA concentration and confirming the expected result obtained from the strip. A known concentration of EDTA was spiked into the control batch of AAT post-production to ensure that none of the components of the AAT would interfere with the validity of the test strips. To perform the test, samples were centrifuged and supernatant was collected and applied to the test strips. Strips were read according to the manufacturer's instructions.

Residual triton X-100 levels in AAT were quantified by reverse phase high-performance liquid chromatography (HPLC). The control batch manufactured without Triton-X100 served as a negative control in these experiments. Triton-X100 standards were prepared in water and run along with the AAT samples. AAT and spiked control samples were prepared for HPLC by repeated centrifugation at >12,000 rpm to remove insoluble proteins and collect aqueous supernatant. Soluble proteins were then precipitated using methanol-chloroform extraction. Both the aqueous and organic layers were collected and combined. The protein pellet was washed with chloroform and the supernatant was also combined with the sample (discarding the protein pellet). Samples were concentrated by freeze-drying in a lyophilizer until completely dry, then resuspended in a consistent volume of pure water for HPLC. An isocratic reverse phase separation was performed

using an HC-C18(2) column and two mobile phases: HPLC-grade water and 100% acetonitrile. The peak corresponding to Triton-X100 was measured and quantified relative to standards.

Statistical Analysis

Statistical analysis was performed using GraphPad Prism software. In grouped analyses with a single variable, significance was determined by one-way analysis of variance (ANOVA) using the Holm-Sidak correction for multiple comparisons where applicable ($\alpha = 0.05$). Significance in grouped analyses with two variables was calculated using two-way ANOVA with Tukey post-hoc testing ($\alpha = 0.05$). P values less than 0.05 were considered statistically significant (* < 0.05, ** < 0.01, *** < 0.001, **** < 0.0001). Plotted values represent the arithmetic or geometric mean (RT-qPCR data only) of the data set. Error bars represent +/- one standard deviation or geometric standard deviation (RT-qPCR only).

RESULTS

Building on previous studies done in the Elisseeff lab which characterized the physical properties of AAT, we initially sought to study the biochemical characteristics of AAT. Biochemical assays performed included an *in vitro* cell migration assay, residual chemicals testing, a lipid content assay, and a collagen content assay. There were two main purposes for collecting this data: to get a better understanding of the biochemical composition and properties of the material, and to start building a database with the goal of understanding the batch–to–batch differences in AAT. This information will help define the expected variability from both tissue donors and from any changes in the manufacturing process, and will be critical for scaling up the manufacturing protocols for later stage clinical trials and eventual commercialization. The biochemical characterizations also allowed us to study how the terminal sterilization process of gamma irradiation might change the properties of the final product.

The *in vitro* cell migration assays were conducted on both irradiated and non-irradiated samples from the human clinical batch (TS-02568) (Figure 1). The results of these assays showed that both the irradiated and the non-irradiated samples of human AAT promote cell migration of ASCs across a transwell membrane. In a pilot experiment, images taken of the transwell membrane showed that the non-irradiated AAT was more likely to stick to the membrane, potentially indicating a difference in mechanical properties. A second assay was performed with the samples centrifuged to remove large chunks that might stick to membrane, thus ensuring migration would only be triggered by interaction with soluble factors. In this second assay, the non-irradiated AAT resulted in slightly less cell migration than the irradiated batch. However, this result

was not statistically significant. Both AAT batches promoted significantly more migration than the negative and buffer controls.

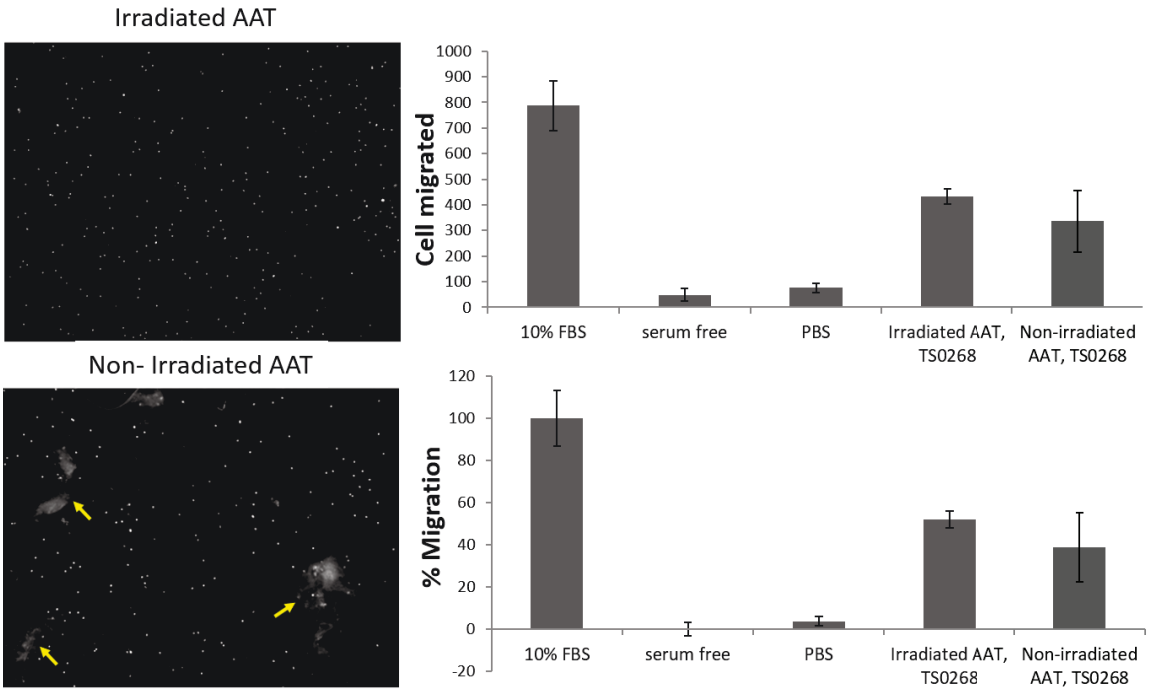

Figure 1. Migration assay results for the clinical batch of human AAT. Microscope images show clumps of non-irradiated AAT stuck to the membrane (arrows), but none for irradiated AAT.

In response to a request from the FDA, assays were developed to monitor the presence of residual process chemicals in the final AAT product (Figure 2). The chemicals of interest were EDTA and Triton X-100, both used during the AAT manufacturing processing. To determine the amount of residual EDTA, Quantofix EDTA test strips were validated using known standards and a spiked control to ensure that none of the components of the AAT would interfere with the validity of the test strips. The results of both validation measures are shown in the picture in Figure 2. The strips indicated that there was no detectable residual EDTA remaining in the final product. This assay was performed on the clinical batch of human AAT.

To test for residual Triton X-100, an HPLC method was developed. This assay determined that there was, on average, 52.524 µg/ml of Triton X-100 remaining in the AAT after processing. This corresponded to a 99.50% removal of Triton X-100 and is well within acceptable safety limits for this chemical.

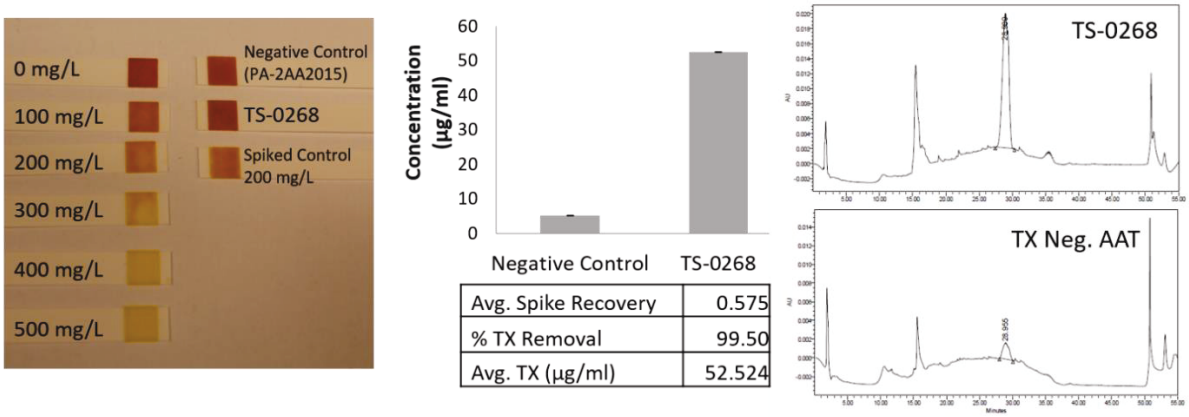

Figure 2. Assays to test the human clinical AAT batch for residual process chemicals. Quantifix EDTA test strips were used to test for EDTA and HPLC was used to test for Triton X-100.

Different key components of the AAT were quantified biochemically. The lipid content assay was performed on a batch of porcine-derived AAT in addition to the human-derived clinical AAT, allowing for an important comparison between lipid removal in these products from two different starting materials. Since the composition and total amount of triglycerides can vary significantly between adipose from different species or potentially even different human donors, it was important to discover if different AAT batches had similar amounts of triglyceride remaining after processing. Since the main type of lipid contained in adipocytes are triglycerides, measurements of glycerol content correspond approximately to total lipid content in these tissues. In both pig and human derived AAT, glycerol content was less than 0.02 µmol/mg of sample (Figure 3A). This is much lower than the glycerol content of adipose tissue, which is 0.7816 µmol/mg sample for adipose tissue harvested from humans and 0.7405 µmol/mg

sample for adipose tissue harvested from pigs. This corresponds to a percent lipid removal of 97.8% for pAAT and an average of 98.6% removal for hAAT. As predicted, irradiation of the AAT does not alter the lipid content.

A hydroxyproline assay determined the collagen content of both the irradiated and non-irradiated clinical batches of hAAT. This assay showed that the irradiated hAAT is 87.0 ± 5.1% collagen by dry weight and non-irradiated hAAT is 89.0 ± 15.1% collagen by dry weight (Figure 3B). Bovine collagen was used as the positive control to validate the assay and was measured to be 100.6 ± 9.1 % collagen. These results are consistent with the measurements found in the literature and are expected due to the relatively high collagen content of most native ECMs.

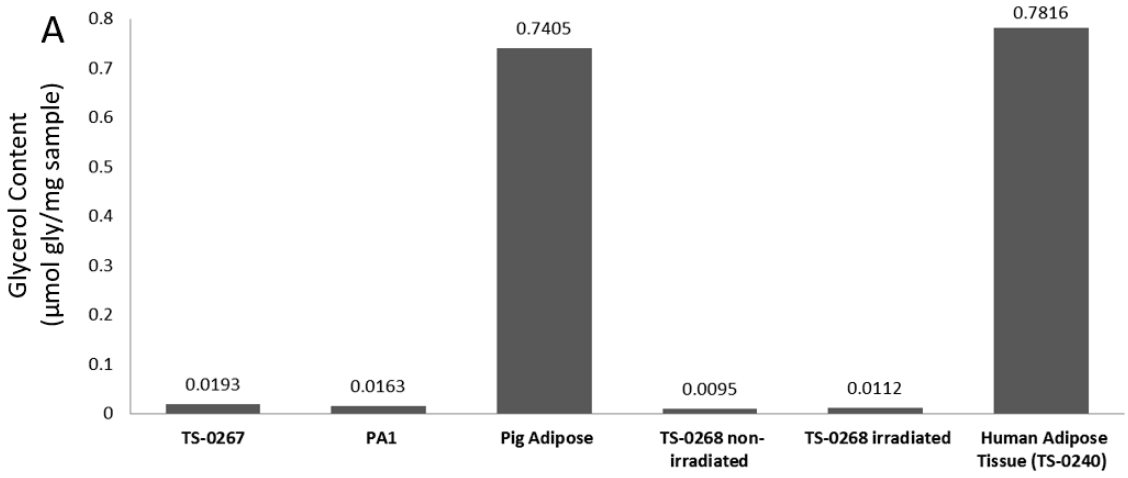

B

Sample	Hydroxyproline (µg/mg of dry sample)	Collagen (µg/mg of dry sample)	Collagen % (dry weight)
Irradiated AAT	110.2 ± 6.5	870.0 ± 51.2	87.0 ± 5.1
Non-irradiated AAT	112.7 ± 19.1	889.9 ± 150.5	89.0 ± 15.1
Bovine Collagen	127.4 ± 11.6	1006.2 ± 91.3	100.6 ± 9.1

Figure 3. Lipid content assay and hydroxyproline assay results. A) Lipid content assay shows the glycerol content of a human lab batch (TS-0267), a pig lab batch (PA1), and both irradiated and non-irradiated human clinical batch (TS-0268) compared to both human and pig adipose tissue. B) Hydroxyproline assay to test collagen content of both the irradiated and non-irradiated human clinical batch (TS-0268).

To assess the *in vivo* response to the material, subcutaneous (SQ) injections of either hAAT or pAAT were made at superior and inferior positions on the dorsal side of the animal. The implants were harvested and analyzed at 1 or 3 weeks to assess short-term and longer term immune cell responses. Histological analysis showed minimal acute inflammatory response at both 1 and 3 weeks (Figure 4). Histological sections also show some significant differences in morphology between the hAAT and pAAT. The pAAT has a more textured appearance with larger pieces of material, while the hAAT looks

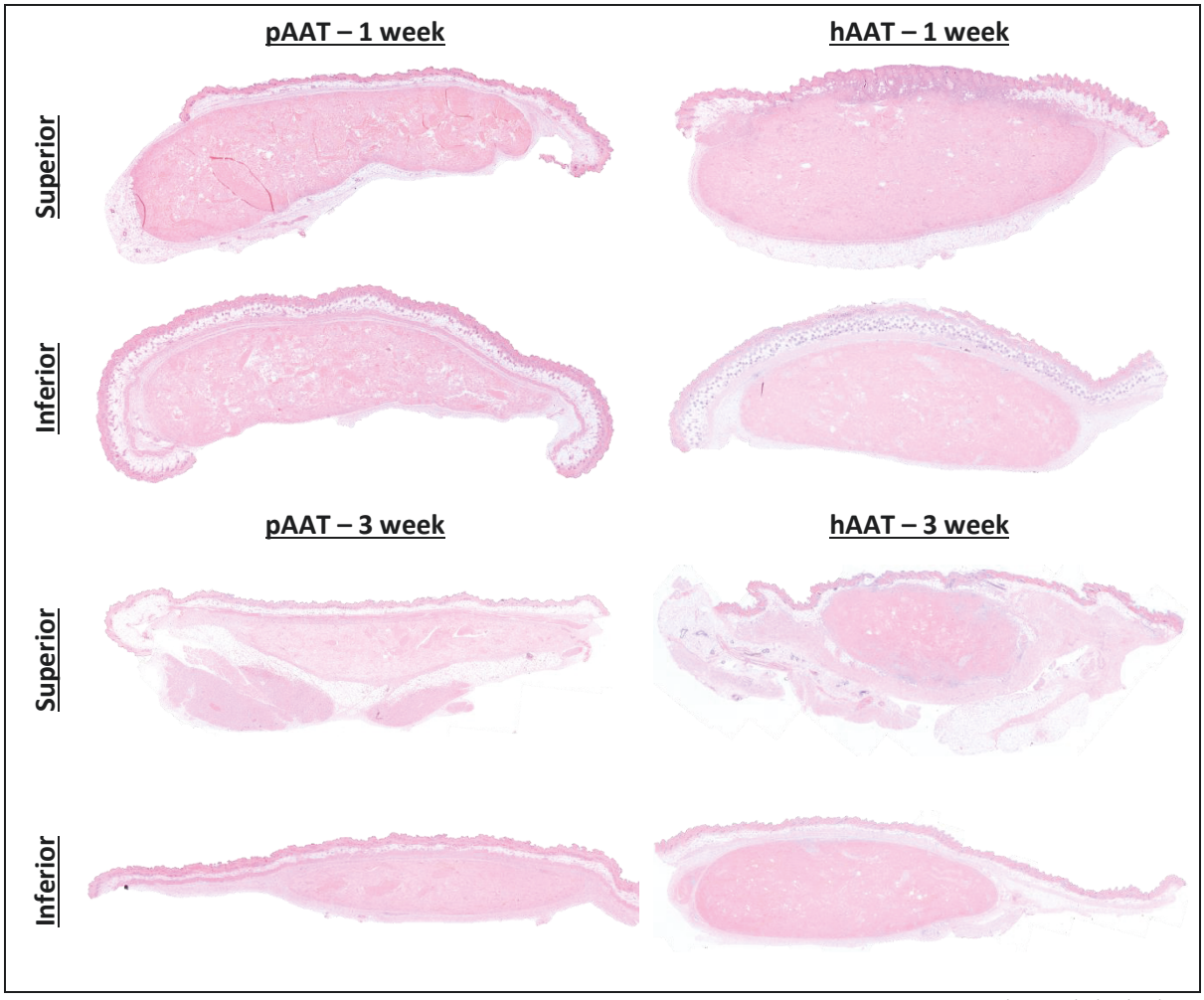

Figure 4. Hematoxylin and Eosin staining of subcutaneous implants. Implants labeled as "top" were injected at a superior position and implants labeled as "bottom were injected at an inferior position.

smoother and more homogenous. Cell infiltration occurs from the surrounding tissues into the implant, indicating that the material promotes cell migration and corroborating the results of the *in vivo* cell migration assay. It is also interesting to note the brown fat pad adjacent to the implant in the superior position (visible in the pAAT 3-week top section) which could potentially impact the cellular response to the material.

The immune cell profile of the subcutaneous implants after 1 or 3 weeks in vivo were assessed using flow cytometry (Figure 5). Overall, the flow analysis showed that human and porcine AAT had similar immune cell profiles at each time point. A greater percentage of the cells migrating into the implant were CD206+ macrophages (M2 polarized) than CD86+ (M1 polarized) macrophages, suggesting that the biomaterial

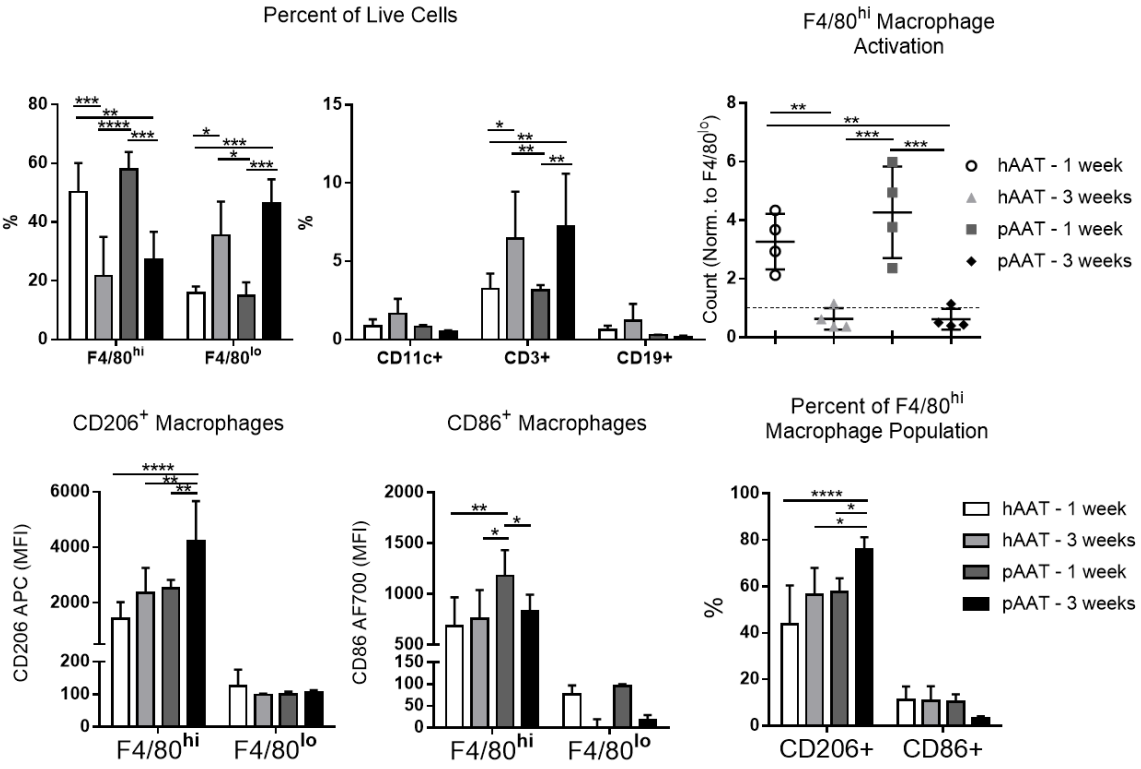

Figure 5. Subcutaneous flow cytometry results at 1 and 3 weeks. Implants were pooled for each animal to ensure adequate cell number for analysis. Statistical significance calculated using two-way ANOVA with TUKEY post-hoc testing for everything except F4/80hi macrophage activation for which a one-way ANOVA with TUKEY post-hoc testing was used. * < 0.05, ** < 0.01, *** < 0.001, **** < 0.0001.

skews macrophage polarization towards an M2 phenotype. When considering this result, it is important to understand that macrophage polarization is spectrum rather than a binary change, so macrophages could potentially be somewhere between an M1 and an M2 phenotype. It was also noted that the level of macrophage activation ($F4/80^{hi}$ relative to $F4/80^{lo}$) was higher at 1 week than at 3 weeks. The percentage of CD3+ T cells in the implant is significantly higher at 3 weeks than at 1 week, indicating that the T cell response begins prior to 1 week and increases to a peak at some later time point.

Gene expression analysis performed on the SQ implants at 3 weeks post-injection showed that *iNos*, an M1 gene, and *Arg1*, an M2 gene, were both significantly increased in almost all of the implants (Figure 6). The increase in *iNos* gene expression in the pAAT far implant was not considered statistically significant. This information is interesting given the higher percentage of CD206+ M2 macrophages than CD86+ M1 macrophages in the implant observed in the flow cytometry data. Other genes including *Il-4* were elevated in the implant relative to normal muscle, but these results were not statistically significant.

A mouse volumetric muscle wound (VML) model was used to study the response to both pAAT and hAAT in a wound environment. In this experiment, a critical sized defect was created in the mouse quadriceps muscle and was filled with a biomaterial or saline as a control. To explore whether there was an effect related to xenogenic AAT in the mouse wound model, these experiments also included mouse-derived AAT produced from C57BL/6 mice as a syngeneic ECM control. Response to the biomaterials was assessed at 1 week post- injury.

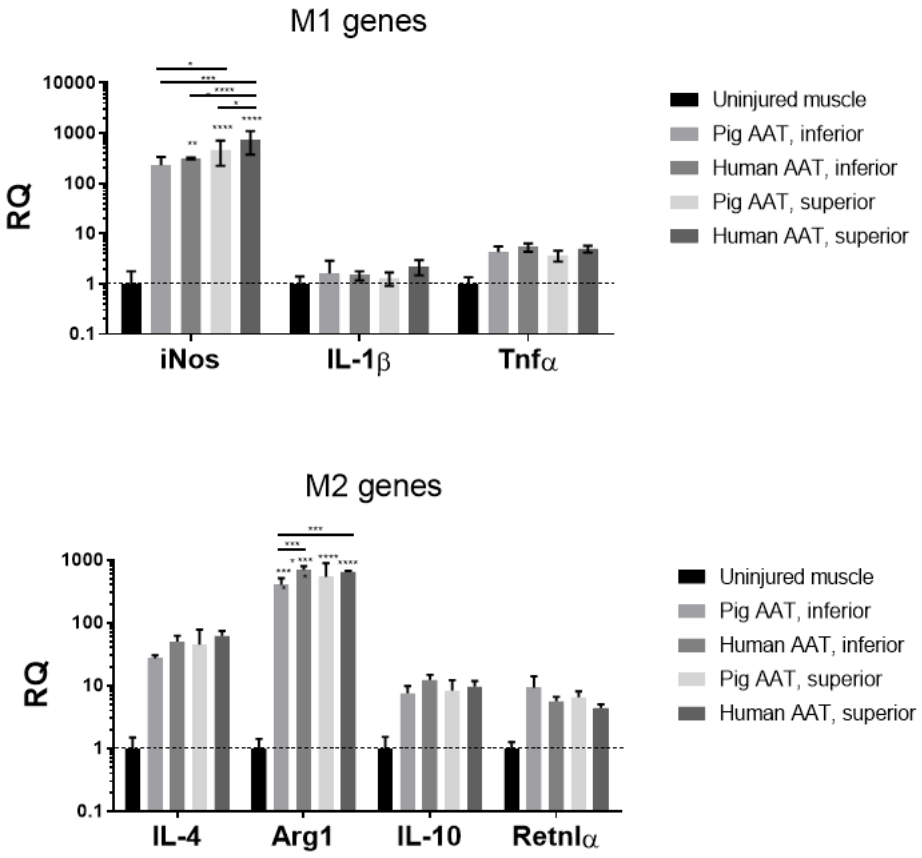

Figure 6. Subcutaneous RT-PCR results at 3 weeks. Implants in the superior position and inferior positions were analyzed separately relative to gene expression in uninjured quadriceps muscle. Significance calculated using two-way ANOVA with TUKEY post-hoc testing. Asterisks with no line indicate significance compared to uninjured. * < 0.05, ** < 0.01, *** < 0.001, **** < 0.0001.

Flow cytometry results of the 1 week VML study included a mouse AAT (mAAT) group to analyze the immune response to a genetically-matched ECM material (Figure 7). There were significantly more immune cells in quadriceps treated with hAAT and pAAT than those treated with mAAT or saline. Overall, the immune cell profile of wounds treated with mAAT more closely resembled those treated with saline than the xenogeneic AAT groups. The percentage of myeloid cells (CD45+CD11b+) was higher

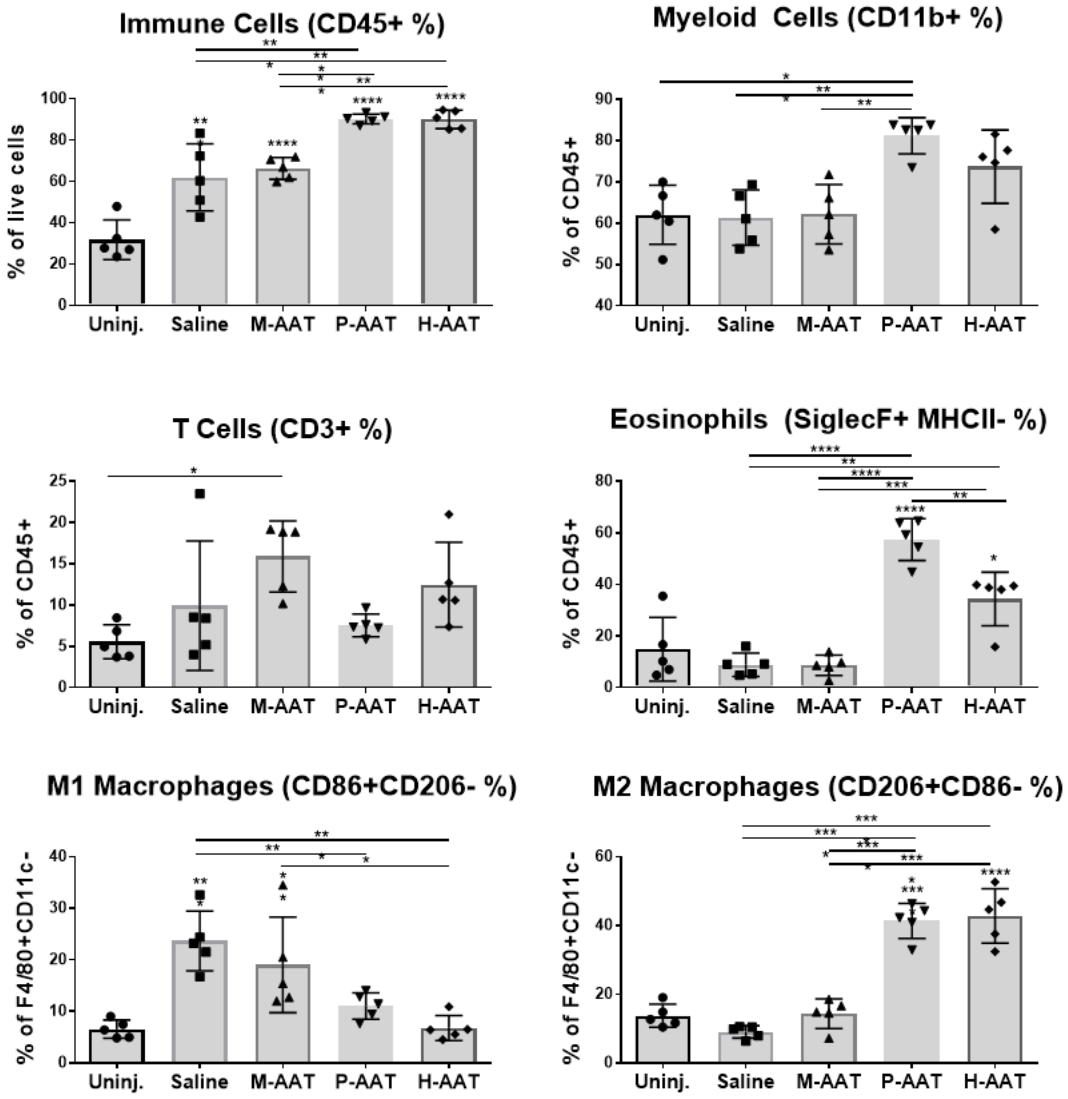

Figure 7. Volumetric muscle loss flow cytometry results at 1 week. Groups labeled as "uninj." are uninjured quads from age-matched animals. Statistical significance calculated using a one-way ANOVA with Tukey post-HOC testing. Significance without lines indicate significance compared to uninjured. * < 0.05, ** < 0.01, *** < 0.001, **** < 0.0001.

in both pAAT and hAAT. The xenogeneic AATs also recruited a much stronger eosinophil response (Siglec-F+MHCII-). Interestingly, wounds treated with mAAT were the only group with a statistically significant increase in the proportion of T cells compared to uninjured quads. However, this there was no significant difference in the absolute number of T cells at the wound site between the different ECM treatments (data

not shown). The data also indicates that pAAT and hAAT promote greater skewing of polarized macrophages to an M2-like phenotype than mAAT, though overall mAAT is still somewhat M2-polarizing. Saline treatment promotes a more M1-like phenotype than any ECM treatment, as determined by the relative proportions of CD206+CD86- and CD86+CD206- macrophages.

RT-qPCR analysis of the wounded muscle 1 week after treatment showed that wounds treated with mouse syngeneic AAT were not significantly different than wounds treated with saline or uninjured muscle in any of the genes tested (Figure 8). Most of these M2 genes - including *Il-4*, *Arg1*, and *Retnlα* - were significantly increased in pAAT and hAAT treated wounds compared to saline treated wounds and uninjured muscle. Increases were also observed in M1 genes relative to saline treatment; though these increases were generally similar between different ECMs. Most importantly, expression of *Il-4* increased more than 100-fold in pAAT and hAAT relative to control groups, whereas mAAT also increased but was not significantly different than saline. Taken together, these results are consistent with flow cytometry analysis of macrophage polarization and indicate a difference in the profile of immune cells migrating to wounds treated with syngeneic ECM than those treated with xenogeneic ECMs.

A human clinical trial studied the safety of AAT when implanted subcutaneously in human participants. The primary outcome measures of this study were histopathology, safety, and patient and physician satisfaction. On an exploratory basis, the immune cell populations and cell migration into the implant were also characterized.

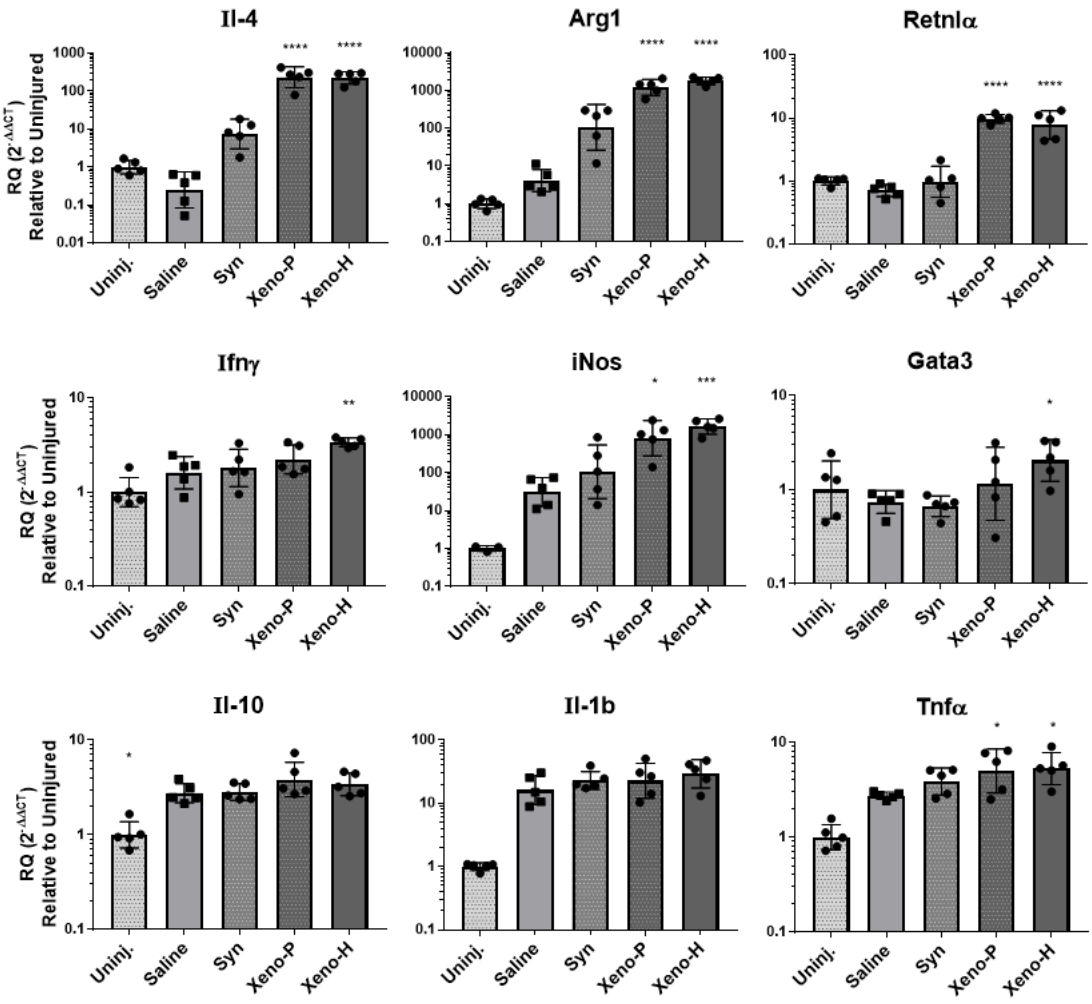

Figure 8. Volumetric muscle loss RT-PCR results at 1 week. Statistical significance is calculated relative to saline controls. * < 0.05, ** < 0.01, *** < 0.001, **** < 0.0001.

Histological analysis of the clinical trial implants showed minimal negative inflammatory response with cell migration into the implant (Figure 10), demonstrating the potential for new tissue formation. The implants also show good volume retention at up to 18 weeks post-injection, the latest time-point studied. The implants do not show any indication of capsule or cyst formation or tissue necrosis. All of these histological results indicate demonstrate the biocompatibility of AAT when implanted into humans and that the implant may support new tissue formation.

Participant	Excision Time Point	Control Tissue	Implant Tissue
001	4 weeks	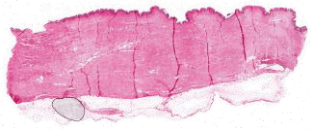	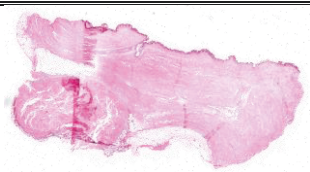
002	2 weeks	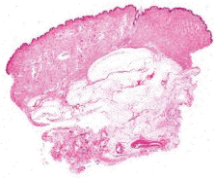	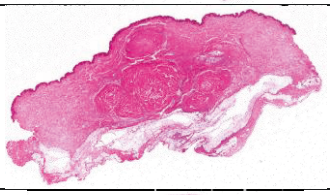
003	1 week	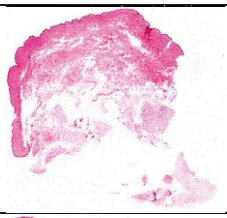	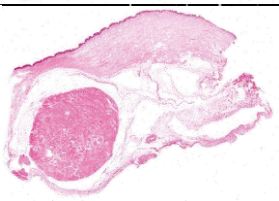
004	2 weeks	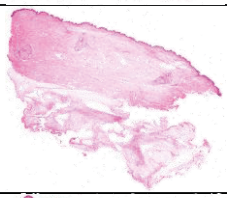	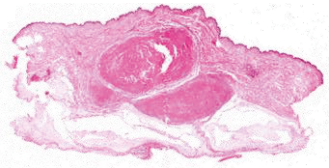
005	4 weeks	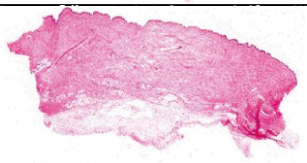	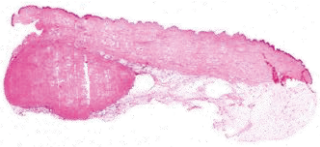
006	1 week	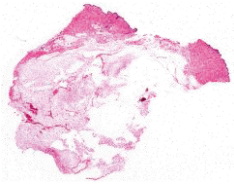	
007	18 weeks	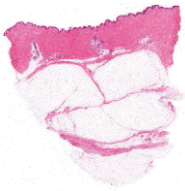	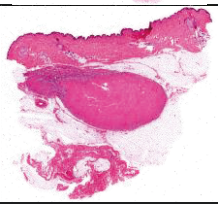
008	6 weeks	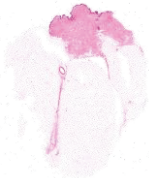	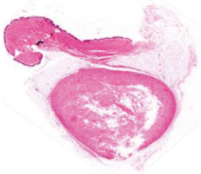

Figure 10. Histological analysis of clinical trial samples. Control tissue is a distal piece of adipose tissue. Implant tissue is AAT implant and surrounding tissue.

Additional clinical safety outcomes were obtained from patient surveys following injection and at follow-up visits. All anticipated adverse events were characterized as mild and were localized to the injection site (Figure 11). Two patients experienced mild pain/tenderness (typically during the injection visit); four patients had mild erythema (reddening of the skin) and/or bruising. Hyperpigmentation was observed in one patient, and textural changes in three patients. Participants were also asked to score their pruritus, (itching) and pain during follow-up visits. On only two occasions, very mild pruritus was reported. No patients reported pain during follow-up visits.

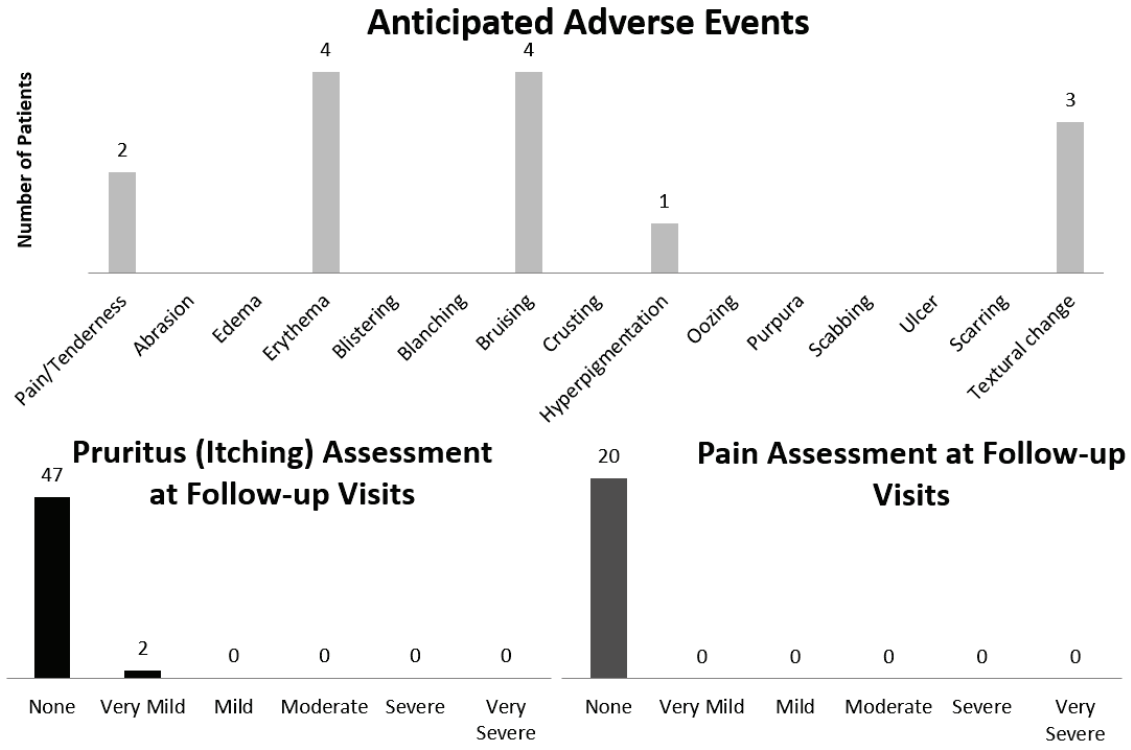

Figure 11. Anticipated adverse events, pruritus, and pain assessments. Participants were asked to score pruritus, or itching, and pain at all appointments including injection and excision appointments.

Participants and physicians also filled out satisfaction and ease-of-use surveys respectively. Participants were asked to rate their comfort both during and 30 minutes after injection and the appearance after injection, including fullness of injection site, softness, smoothness, and naturalness (Figure 12). Physicians were asked to rate their satisfaction with the ease of use, fullness of injection site, and overall appearance and the appearance of the implant, including softness, smoothness, and naturalness (Figure 13). Most of the participants reported being somewhat or very satisfied with their comfort during and after the injection. No participant reported being dissatisfied with the fullness of the injected site. Participant appearance ratings varied with most of the patients reporting that the implant felt very soft, very smooth, and very natural.

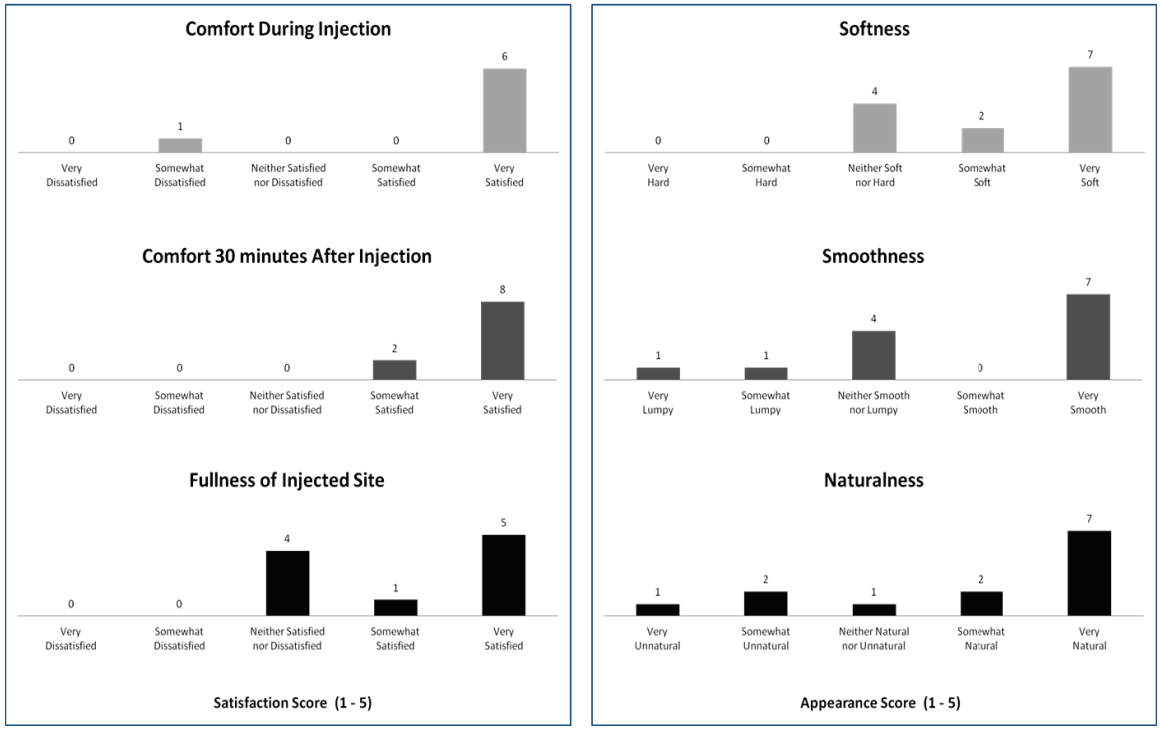

Figure 12. Participant satisfaction surveys.

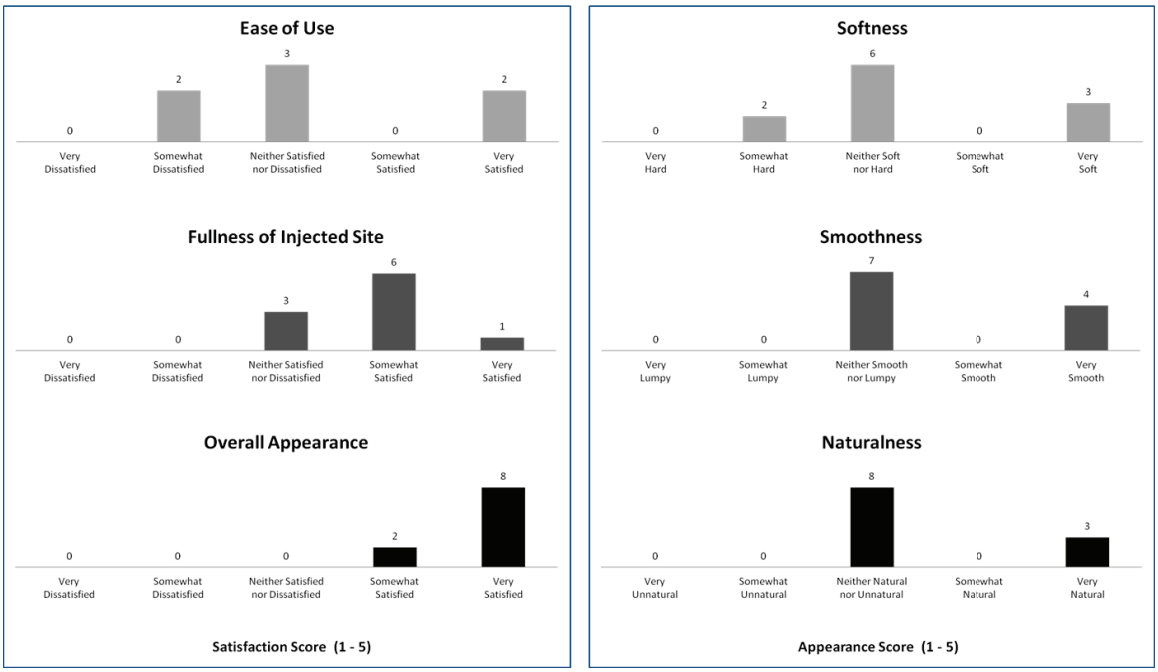

Figure 13. Physician satisfaction surveys.

No serious adverse events (SAE) were reported related to the study (Table 4). One patient was hospitalized for an infection following procedure, but this event was determined to be unrelated to the material and a result of the patient's poor overall health. Panel reactive antibody (PRA) testing showed that exposure to AAT did not significantly increase Immunoglobulin G (IgG) HLA antibodies at either 4 or 12 weeks post-injection for 7 out of 8 participants (Table 5). One participant had a minor increase in IgG HLA antibodies at 12 weeks post-injection, but this was considered not clinically relevant. The PRA testing results indicated that there was no systemic reaction to the AAT.

Taken together, the clinical trial results indicate that the product is safe for use in humans. All of the adverse events recorded were mild and expected. No serious adverse events related to the study were reported. Exposure to the product did not cause a systemic reaction. Both physicians and participants showed neutral to good satisfaction with the product including comfort for the participants, ease of use for the

Table 4. Serious adverse events.

PT #	Excision Time point	SERIOUS ADVERSE EVENTS
003	1 week	None
006	1 week	None
002	2 weeks	None
004	2 weeks	None
005	4 weeks	None
001	4 weeks	None related to study*
008	6 weeks	None
007	18 weeks	None

*Patient 001 underwent treatment for a severe infection following the panniculectomy procedure. The injection occurred after the removal of the AAT implant and the medical monitor deemed that this SAE was a result of the surgical procedure only and related to the patient's poor overall health and other co-morbidities.

Table 5. Panel Reactive Antibody test results.

PT #	Excision Time point	BASELINE TESTING	POST-INJECTION TESTING	
			Increase in IgG HLA antibodies at....	
		IgG HLA Positive?	*4 weeks?*	*12 weeks?*
003	1 week	Yes	No	No
006	1 week	No	No	Yes; lowest antibody detection level, CPRA $_{Low}$ = 44
002	2 weeks	Participant withdrew		
004	2 weeks	Yes	No	No
005	4 weeks	No	No	No
001	4 weeks	No	No	No
008	6 weeks	No	No	No
007	18 weeks	Yes	No	No

physicians, and overall appearance and feel of the implant. The results of the histological analysis also indicate that the product is safe for use in humans and retains its volume for up to 18 weeks. Importantly, the histological analysis also shows that the product promotes cell migration and so has the potential to promote new tissue formation and permanent correction of soft tissue defects.

DISCUSSION

Preclinical studies showed promising results for the safe and effective use of AAT for soft tissue reconstruction in humans. In both VML and subcutaneous studies in mice, AAT demonstrated good tissue integration with cell migration into the implant. No significant inflammatory response was noted in these experiments. Results obtained from the subcutaneous implants indicate that macrophages begin migrating in from the surrounding tissue within 1 week. By three weeks, however, the macrophages are no longer as dominant and adaptive cells such as T cells have begun to appear. This mimics the immune response to a wound during which macrophages enter the wound first followed by lymphocytes [18]. RT-qPCR analysis showed an increase in gene expression for both *iNos*, the inducible form of nitric oxide synthase, and *Arg1*, Arginase 1. The *iNos* gene generates nitric oxide and is an important enzyme in the macrophage inflammatory response [27]. *Arg1* is an enzyme that metabolizes arginine and is highly expressed on M2 macrophages. Resident adipose tissue-associated macrophages typically have M2-like polarization and express *Arg1* and are important for balancing inflammation in fat tissue and maintaining metabolism. Interestingly, *Arg1* and *iNos* compete to metabolize arginine when they are co-expressed [28]. The co-expression of *iNos* and *Arg1* likely indicates that the macrophages present within the AAT at 3 weeks are neither purely M1 nor M2, though they may be skewed towards M2 at a population level.

Flow cytometry analysis of the AAT-treated quadriceps muscles at 1 week after critical injury showed significant infiltration of immune cells into the wound site. Overall the flow data suggest similarity between the xenogeneic AATs, including an increased percentage of recruited immune cells (CD45+), eosinophils (CD45+ CD11b+ SiglecF+

MHCII-), and M2 macrophages (CD206+CD86-) relative to saline and uninjured controls. Although the differences were not significant, syngeneic mouse AAT was also somewhat more M2-polarizing than saline alone, and recruited greater percentages of immune cells. However, the macrophages present in mouse AAT tended to be more M1-polarized (CD86+) than in the other AATs. Gene expression analysis also showed that significantly more interleukin 4 (*Il-4*) was present in wounds treated with both pig and human AAT than those treated with saline or mouse AAT. This indicates that in some contexts, AAT promotes the migration of immune cells which trigger the release of this key pro-regenerative cytokine. This increased expression of *Il-4* is not correlated with an increase in the proportion or absolute number of T cells in the wound, but may be due to the increased activity of myeloid cells orchestrating the upregulation of *Il-4*. Missing from these analyses are quantifications of different T cells subsets, particularly T_H2 helper T cells, which are essential for creating a pro-regenerative microenvironment.

The combined results of our syngeneic versus xenogeneic AAT studies indicate that pro-regenerative immune responses to ECM are likely not driven by non-specific damage-associated molecular patterns (DAMPs) inherent to all ECMs [29]. It is possible that a response related to foreign antigens in both the pig and human AAT is significantly driving the observed increases in *Il-4* expression, eosinophils, or M2 macrophage polarization. However, there are likely factors other than species contributing to the differences observed between AAT treatments. Biochemical characterizations of the mouse AAT may reveal a key difference that helps to explain the loss of the pro-regenerative phenotype. More rapid resorption of the mouse AAT compared to the xenogeneic materials may also be preventing the immune system from mounting a full

M2/Th2 response. Additional studies will be needed to confirm the mechanism or mechanisms driving these phenotypes. Future work will investigate an allogeneic ECM material in the wound environment in order to better understand the implications of these results for the translation of AAT to clinical applications.

In Phase I clinical trial studies, AAT proved safe, biocompatible, and well-tolerated by all outcomes measured. No serious adverse events were reported, and all anticipated adverse events were mild and localized to the injection site. Both physicians and participants reported overall satisfaction with the comfort/ease of use and appearance of the injected area. Importantly, implant volume was retained until the latest measured time point of 18 weeks, and the material integrated into the surrounding tissue rather than becoming isolated by fibrosis. Histological analysis of the implants also showed significant cell migration into the implant from surrounding tissue which generally increased as time went on. Although immune cells were observed within the implant, the lack of a systemic immune reaction suggests that any immune-modulation is occurring locally. All of this data indicates that AAT is safe for use in humans and has the potential to support cell infiltration and new tissue formation. Future analyses will be conducted to identify specific types of immune cells present in the AAT. It will be critical to determine whether these cells are pro-inflammatory immune cells, pro-regenerative immune cells, or stem cells to fully understand the cellular response to the material.

CONCLUSION AND FUTURE WORK

This work describes the development of an adipose-tissue derived ECM material for soft tissue reconstruction, including many of the material characterizations and preclinical studies that lead to the first in human study. These preclinical results and others were critical in obtaining FDA approval for initial clinical testing. Consequently, the safety results obtained from this first clinical study will be leveraged to advance AAT to Phase II clinical testing to confirm safety and determine efficacy in patients. Our most recent animal studies have sought to identify the mechanisms of ECM-mediated immunomodulation and will be critical to help define clinical indications for AAT and inform future research.

In these preclinical studies, AAT demonstrated volume retention, significant tissue integration, and minimal inflammation. Subcutaneous implants attracted large proportions of macrophages around 1 week, followed later by the clearing of the macrophages and increased migration of T cells. In a mouse wound environment, pig and human AAT elicited a strong M2-macrophage response while syngeneic mouse AAT elicited a more neutrally-polarized macrophage response that was similar to saline treated wounds. However, CD3+ T cell response was not significantly impacted by ECM tissue source, which may suggest a combination of factors (both species-specific and non-species specific properties of ECMs) is responsible for the immune response to these materials. The ability of AAT to modulate immune response and induce a favorable pro-regenerative environment could potentially be harnessed to improve wound healing and reduce scarring after injury. This data indicates that AAT could be a good substitute for autologous fat transfer in the treatment of soft tissue defects.

Future studies will determine the immune response to allogeneic ECM in a wound model and determine mechanisms contributing to the ECM-associated immune microenvironment. Biochemical characterizations will continue for each new manufactured lot to form an understanding of batch-to-batch variability and help determine which properties of the material are correlated with successful clinical outcomes. These factors and others will be considered for design and validation of a scaled-up manufacturing process for future clinical trials involving significantly more participants. Together, this work will enable Phase II clinical testing, which will be conducted to test the safety and efficacy of AAT in filling small soft tissue defects in human patients.

REFERENCES

1. Ring, A., et al., *Reconstruction of Soft-Tissue Defects at the Foot and Ankle after Oncological Resection.* Frontiers in Surgery, 2016. **3**(15).
2. Coleman, S.R., *Structural fat grafting: more than a permanent filler.* Plast Reconstr Surg, 2006. **118**(3 Suppl): p. 108S-120S.
3. Ross, R.J., et al., *Autologous fat grafting: current state of the art and critical review.* Ann Plast Surg, 2014. **73**(3): p. 352-7.
4. Rubin, J.P. and K.G. Marra, *Soft Tissue Reconstruction*, in *Adipose-Derived Stem Cells: Methods and Protocols*, J.M. Gimble and B.A. Bunnell, Editors. 2011, Humana Press: Totowa, NJ. p. 395-400.
5. Rai, S., A.M. Marsland, and V. Madan, *Facial Fat Necrosis Following Autologous Fat Transfer and its Management.* Journal of Cutaneous and Aesthetic Surgery, 2014. **7**(3): p. 173-175.
6. Wainwright, D.J., *Use of an acellular allograft dermal matrix (AlloDerm) in the management of full-thickness burns.* Burns, 1995. **21**(4): p. 243-248.
7. Gilbert, T.W., T.L. Sellaro, and S.F. Badylak, *Decellularization of tissues and organs.* Biomaterials, 2006. **27**(19): p. 3675-3683.
8. Frantz, C., K.M. Stewart, and V.M. Weaver, *The extracellular matrix at a glance.* Journal of Cell Science, 2010. **123**(24): p. 4195-4200.
9. Hinderer, S., S.L. Layland, and K. Schenke-Layland, *ECM and ECM-like materials — Biomaterials for applications in regenerative medicine and cancer therapy.* Advanced Drug Delivery Reviews, 2016. **97**: p. 260-269.
10. Hoshiba, T., et al., *Decellularized matrices for tissue engineering.* Expert Opinion on Biological Therapy, 2010. **10**(12): p. 1717-1728.
11. Coelho, M., T. Oliveira, and R. Fernandes, *Biochemistry of adipose tissue: an endocrine organ.* Archives of Medical Science : AMS, 2013. **9**(2): p. 191-200.
12. Tran, T.T. and C.R. Kahn, *Transplantation of adipose tissue and stem cells: role in metabolism and disease.* Nat Rev Endocrinol, 2010. **6**(4): p. 195-213.
13. Coleman, S.R., *Structural Fat Grafting: More Than a Permanent Filler.* Plastic and Reconstructive Surgery, 2006. **118**(3S): p. 108S-120S.
14. Gallagher, D., et al., *Healthy percentage body fat ranges: an approach for developing guidelines based on body mass index.* Am J Clin Nutr, 2000. **72**(3): p. 694-701.
15. Rehman, J., et al., *Secretion of angiogenic and antiapoptotic factors by human adipose stromal cells.* Circulation, 2004. **109**(10): p. 1292-8.
16. Ouchi, N. and K. Walsh, *Adiponectin as an anti-inflammatory factor.* Clinica Chimica Acta, 2007. **380**(1–2): p. 24-30.
17. Ferrante, A.W., Jr., *The immune cells in adipose tissue.* Diabetes Obes Metab, 2013. **15 Suppl 3**: p. 34-8.
18. Park, J.E. and A. Barbul, *Understanding the role of immune regulation in wound healing.* The American Journal of Surgery, 2004. **187**(5, Supplement 1): p. S11-S16.
19. Wynn, T.A., A. Chawla, and J.W. Pollard, *Macrophage biology in development, homeostasis and disease.* Nature, 2013. **496**(7446): p. 445-55.

20. Sadtler, K., et al., *Developing a pro-regenerative biomaterial scaffold microenvironment requires T helper 2 cells.* Science, 2016. **352**(6283): p. 366-70.
21. Brown, B.N., et al., *Macrophage phenotype as a predictor of constructive remodeling following the implantation of biologically derived surgical mesh materials.* Acta Biomater, 2012. **8**(3): p. 978-87.
22. Gordon, S. and P.R. Taylor, *Monocyte and macrophage heterogeneity.* Nat Rev Immunol, 2005. **5**(12): p. 953-64.
23. Adamson, R., *Role of macrophages in normal wound healing: an overview.* J Wound Care, 2009. **18**(8): p. 349-51.
24. Wu, I., et al., *An injectable adipose matrix for soft-tissue reconstruction.* Plast Reconstr Surg, 2012. **129**(6): p. 1247-57.
25. Wu, I., *Design and translation of an adipose-derived soft tissue substitute*, in *Biomedical Engineering*. 2014, Johns Hopkins University: Baltimore.
26. Pulagam, S.R., T. Poulton, and E.P. Mamounas, *Long-term clinical and radiologic results with autologous fat transplantation for breast augmentation: case reports and review of the literature.* Breast J, 2006. **12**(1): p. 63-5.
27. McNeill, E., et al., *Regulation of iNOS function and cellular redox state by macrophage Gch1 reveals specific requirements for tetrahydrobiopterin in NRF2 activation.* Free Radical Biology and Medicine, 2015. **79**: p. 206-216.
28. Murray, P.J., *Amino acid auxotrophy as a system of immunological control nodes.* Nat Immunol, 2016. **17**(2): p. 132-139.
29. Sofat, N., et al., *Interaction between extracellular matrix molecules and microbial pathogens: evidence for the missing link in autoimmunity with rheumatoid arthritis as a disease model.* Frontiers in Microbiology, 2014. **5**: p. 783.

CURRICULUM VITAE

Education

Johns Hopkins University, Baltimore, MD May 2017
Master of Science in Engineering in Biomedical Engineering

Villanova University, Villanova, PA May 2015
Bachelor of Science in Chemical Engineering
Minors in Bioengineering and Mathematics

Research Experience

Graduate student researcher, **Laboratory of Dr. Jennifer Elisseeff**, Johns Hopkins
August 2015-May 2017
Use techniques such as flow cytometry, RT-PCR, cell culture, and histology to test a decellularized adipose extracellular matrix product in various animal models to determine the effectiveness, safety, and immune modulatory properties of the product. Assist in the execution of the Phase I and the planning of the Phase II clinical trial studies for the product, including preparation of regulatory documents. Optimize production protocols and design quality control testing for the product. Analyze and organize data for use in presentations, manuscripts, and regulatory documents. Prepare grant applications.

Explore the ability of a biomaterial scaffold to modulate the tumor immune microenvironment. Evaluate the role of the immune system on the growth of cancer in an animal model. Analyze the effect of drug administration on the response to the biomaterial and the growth of cancer.

Research Assistant, **Invisible Sentinel,** Philadelphia, PA
May 2015-August 2015
Assisted in the development and validation of a new assay, including testing limit of detection and inclusivity/exclusivity. Tested and validated new technology to be used with a company product. Assisted with cell culture, inventory, and other laboratory projects.

Undergraduate student researcher, **Biomaterials and Drug Delivery Laboratory,** Villanova University
August 2014-May 2015
Conducted laboratory experiments to develop effective routes of targeted drug delivery to the lungs using nanoparticles. Synthesized PLA-PEG copolymer micelles in which to encapsulate a drug to treat severe asthma. Optimized polymer synthesis protocols.

Research Intern, **Invisible Sentinel,** Philadelphia, PA
May 2013-August 2013
Developed a pure positive control for a company product by sequencing and cloning strands of DNA. Created a database of different strains of bacteria to be used by the company. Assisted with various research projects in a laboratory setting.

Teaching Experience

Grader, **Johns Hopkins University,** Baltimore, MD
Course: Statistical Mechanics and Thermodynamics
Fall 2015, Fall 2016
Course: Models and Simulations
Spring 2015, Spring 2016

Teaching Assistant, **Villanova University,** Villanova, PA
Course: Freshman Miniproject: Artificial Kidney
October 2013-May 2015

Conference Presentations

A.J. Parrillo, BS, A.E. Anderson, BS, I. Wu, PhD, K. Sadtler, PhD, L. Chung, BS, C. Cooney, MPH, D. Cooney, MD, PhD, R.M. Payne, BS, J. Aston, BS, P. Byrne, MD, J.H. Elisseeff, PhD. **An Adipose Tissue Extracellular Matrix Derived Biomaterial for Soft Tissue Reconstruction**. *Northeast Bioengineering Conference.* Newark, NJ. March 31, 2017-April 2, 2017